

# Blends of Thermoplastic Polyurethanes and Polyamide 12: Structure, Molecular Interactions, Relaxation, and Mechanical Properties

S. S. PESETSKII,<sup>1</sup> V. D. FEDOROV,<sup>1</sup> B. JURKOWSKI,<sup>2</sup> N. D. POLOSMAK<sup>1</sup>

<sup>1</sup> V. A. Belyi Metal-Polymer Research Institute of National Academy of Sciences of Belarus, 32a Kirov Street, 246652 Gomel, Belarus

<sup>2</sup> Division of Plastic and Rubber Processing, Institute of Materials Technology, Poznan University of Technology, 60-965 Poznan, Poland

Received 30 July 1998; accepted 31 December 1998

**ABSTRACT:** Studies were done to understand the effects of polyamide 12 (PA 12) incorporation on microphase separation (microsegregation) in thermoplastic polyurethanes (TPU) based on oligoether (polytetramethylene oxide, molecular weight, 1000) and oligoester (polyethylene butylene glycol adipate, molecular weight, 2000), and relaxation transitions, compatibility, and molecular interaction energy in polymer blends. It was learned that the addition of PA 12 caused partial degradation of the domain structure in the oligoester-containing polyurethane, whereas interaction of hard blocks in the oligoether-containing polyurethane increased. Analyzing compatibility and interphase interactions in blends is possible in the frame of the quantum theory of relaxation processes. Also, interferences of the components on characteristic temperatures of relaxation transitions were studied. Partial compatibility was detected between PA 12 and the soft block of oligoether-based TPU over the whole range of components concentrations tested. For oligoester-based TPU, partial compatibility was observed only at low polyamide concentrations (up to 20 wt %). Effects of a polyurethane phase on PA 12 crystallization in the blends along with the pattern of concentration—mechanical properties dependencies are discussed. © 1999 John Wiley & Sons, Inc. *J Appl Polym Sci* 74: 1054–1070, 1999

**Key words:** polyurethane; polyamide 12; microsegregation; segmental mobility; Kuhn's segment; molecular interaction

## INTRODUCTION

In recent years, a considerable interest has been shown in the study of blended systems of thermoplastic polyurethanes (TPU) with plastomers.<sup>1–8</sup>

This interest was caused by potentialities of widening the range of polyurethane-based raw materials available where polyurethane of a single grade is used. On the other hand, physical chemists dealing with dissimilar polymers face the necessity of handling problems resulting from specific structures of polyurethane macromolecules, interphase interactions, and microphase transformations in blended systems based on polyurethanes.

One of the most important factors affecting the properties of TPU having block structures that

---

Correspondence to: B. Jurkowski.

Contract grant sponsor: Fundamental Research Foundation of Belarus Republic; contract grant number: X-97/398.

Contract grant sponsor: Polish State Committee of Scientific Research; contract grant number: 7T08 E 01411.

*Journal of Applied Polymer Science*, Vol. 74, 1054–1070 (1999)

© 1999 John Wiley & Sons, Inc.

CCC 0021-8995/99/051054-17

consist of soft (polyester or polyether) and hard (diisocyanate diol) blocks (segments) is thought to be a clear microphase separation (microsegregation) taking place in them. The hard blocks of molecules are connected with each other by intermolecular hydrogen bonding and form domains to act as junctions of physical crosslinking for the soft blocks.<sup>9,10</sup> In providing a network of physical junctions in TPU, the decisive role is played by hydrogen bonds, which are labile, and thus can be redistributed depending on thermal effects or owing to modifications.<sup>9,11,12</sup> The hydrogen bonds distribution influences the extent of microsegregation in TPU and the set of properties typical of these materials. It was supposed that properties of blended systems of TPU with other polymers would depend on how the added polymer influences the extent of microsegregation of polyurethane. It seems useful to study the role of added polymers—modifiers in which hydrogen bonding is the dominating intermolecular process. Aliphatic polyamide belongs to this group of materials. Despite a considerable interest toward TPU/polyamide blends, however, the problems related to specific features of a phase—structural transformations, molecular interactions, viscoelastic behavior of blends and compatibility—have not been investigated adequately. This study was undertaken to treat the above problems as applied to TPU/PA 12 blends.

## EXPERIMENTAL

### Materials

The study was made using polyurethane thermoplastic elastomers (TPU 1 and TPU 2) supplied by Polimersintez Corp. (Vladimir, Russia). Soft TPU blocks were formed by oligoester or oligoether, whereas hard blocks were formed by 4,4'-diphenylmethane diisocyanate and 1,4-butane diol (Table I). The molecular weight of the soft polyether block in TPU 1 was 1000 that of a polyethylene butylene glycol adipate block of oligoester; TPU 2 was 2000. The solubility parameters of TPU blocks were calculated.<sup>13</sup>

The second component of the blends was PA 12 (molecular weight,  $2.7 \times 10^4$ ; melting temperature, 179°C) supplied by Ural Plastik Corp., Ekaterinburg, Russia.

The blends were prepared by mechanically mixing PA 12 and TPU pellets with subsequent extrusion of the dry blend by using the twin-screw

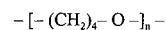
**Table I Characteristics of Virgin Polymers Used for Blend Preparation**

Polymer	Unit Formula	Hard Block Concentration (wt %)	Solubility Parameter [(MJ/m <sup>3</sup> ) <sup>0.5</sup> ]
TPU 1	Soft block I	38.3	15.6
	Hard block II		25.0
TPU 2	Soft block III	38.8	19.1
	Hard block IV		23.1
PA 12	Hard block V		20.3

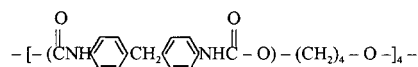
TPU, thermoplastic polyurethanes. Formulas (I–IV) are given below.

#### TPU 1 :

Soft block

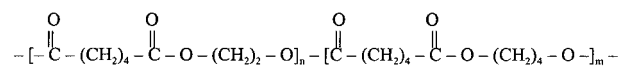


Hard block

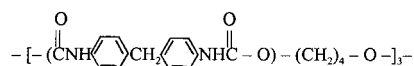


#### TPU 2 :

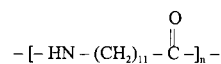
Soft block



Hard block



#### PA 12



Plasticator based on the ZSK-40 extruder (Werner and Pfleiderer, Stuttgart, Germany); the extrudate was cooled and pelletized. The discharge zone temperature was 195°C. The granulate was hot molded to produce films of about 20 to 25  $\mu\text{m}$  in thickness. These were used to take IR absorbency spectra and for the dynamic scanning calorimetry (DSC) analysis. Test samples as plates, size 60  $\times$  5  $\times$  1 mm, also were prepared to

evaluate relaxation spectra using the reverse torsion pendulum device. In addition, virgin homopolymers were molded to obtain films of about 60  $\mu\text{m}$  in thickness to be used in the experiments with "optical blends" of components.

## CHARACTERIZATION

### IR Spectroscopy

IR spectroscopy was used to analyze microsegregation and redistribution of labile hydrogen bonds in TPU when mixed with PA 12. Like other research, we used the absorption band of amide one (A1) referring to the valence vibrations of C=O carbonyl groups and the band of the valence vibrations of NH group ( $\nu\text{NH}$ ) at wave number 3300  $\text{cm}^{-1}$ , as the absorption bands are sensitive toward hydrogen bond formation.<sup>12,14,15</sup> When hydrogen bonds were formed, these bands shift to the lower-frequency region; the shift value depends on the hydrogen bond's energy. The concentrations of associated end free NH groups found in TPU of different compositions showed that most amine groups ( $\geq 80\%$ ) were associated.<sup>11,12</sup> The  $\nu\text{NH}$  vibrations, however, did not allow identification of the hydrogen bonds of different types. Most informative data could be obtained by analyzing the A1 band.<sup>15</sup>

IR spectra were recorded using polymer blends (absorption spectra of the films prepared by molding granulated materials) and model "optical blends." For optical blends, TPU and PA 12 films were placed onto the work surfaces of the cell intended for multiple violated complete internal reflection (MVCIR) (germanium crystal; incidence angle 35°; reflection number, 24). The component concentrations in the optical blends were varied by changing the contact surface area between PA 12 films and MVCIR cell, whereas the contact surface area of TPU films was kept constant. The light-beam penetration depth calculated at 1600  $\text{cm}^{-1}$  was about 0.6  $\mu\text{m}$ . IR spectra were recorded by using spectrophotometer M-80 (Karl Zeiss, Jena, Germany).

### Dynamic Mechanical Spectroscopy

Dynamic mechanical properties were studied by using the reverse torsion pendulum tester with a vibration frequency of 1 Hz. To increase the device sensitivity when analyzing the low-temperature transitions and to detect the small-scale seg-

mental mobility, the plate-like specimens described above were used. Wedge-like undercuts were made in the middle of them. The distance between the clamps was 50 mm. The specimens had the cross-section area 1.7  $\text{mm}^2$  in the undercut region. The pendulum swing angle was about 3°. The counter weight was so chosen that the tensile load would be 3g, which value corresponded to a mean stress of  $1.8 \times 10^{-2}$  MPa. The relative strain caused by the longitudinal stress would not exceed  $10^{-4}$  to  $10^{-5}$  for the materials whose elastic moduli were between 500 and 5000 MPa, and did not influence the dynamic moduli of elasticity measured at shearing ( $G$ ). The maximum average relative strain at shearing did not exceed  $10^{-2}$ . The values of  $G$  and the mechanical loss tangent ( $\tan\delta$ ) were measured within the temperature interval from  $-160$  to  $+180^\circ\text{C}$ . The temperature was maintained within  $\pm 0.5^\circ\text{C}$  accuracy; deviations in  $G$  measurements were 3 to 5%. The dynamic segment  $M_e$  was found using the following expression<sup>16</sup>:

$$M_e = \rho RT/G \quad (1)$$

where  $\rho$  is the polymer density,  $G$  is the dynamic modulus of elasticity at shearing found in the low-temperature plateau region or in the high-elasticity plateau,  $T$  is the temperature, and  $R$  is the gas constant.

The mol energy of interaction for the blend, in the plateau regions of  $G$ -modulus was calculated from the expression<sup>17,18</sup>:

$$E_{i\ bl} = \frac{G_{bl}(\varphi_1 V_1 + \varphi_2 V_2)}{2} \quad (2)$$

where  $E_{i\ bl}$  is the mol energy of interaction in the blend;  $V_1$  and  $V_2$  are, respectively, the reduced mol volumes of components 1 and 2 which make the blend;  $\varphi_1$  and  $\varphi_2$  are the volumetric shares of the components (or TPU blocks); and  $G_{bl}$  is the dynamic modulus of elasticity of the blend at shearing.

The values of  $E_{i\ bl}$  were compared with the reduced cohesive energy of the blend:

$$E_{coh\ bl} = \varphi_1 E_1 + \varphi_2 E_2 \quad (3)$$

where  $E_{coh\ bl}$ ,  $E_1$ , and  $E_2$  are the reduced cohesive energy of the blend and components 1 and 2, respectively.

The criterion  $zG_3^{19}$  was used to evaluate the interphase interaction in the blends:

$$zG_3 = G_{bl} - (\varphi_1 G_1 + \varphi_2 G_2) \quad (4)$$

where  $G_1$  and  $G_2$  are the values of dynamic shear moduli of the blended components, being the difference between the  $G_{bl}$  experimental value and the sum of the additive contributions of each component of the blend.

For incompatible systems with weak or repulsive interactions  $zG_3 < 0$ ; at high negative values there was observed separation in the blend system. If  $zG_3 > 0$ , an active interaction of the blend's components may take place. The concentration–shear elastic modulus dependence for the blend with the two-phase continuity was described using Davies equation<sup>20</sup>:

$$G_{bl}^{1/5} = \varphi_1 G_1^{1/5} + \varphi_2 G_2^{1/5} \quad (5)$$

Deviation ( $\Delta$ ) from Davies equation was found as follows:

$$\Delta = \frac{G_{bl}^{1/5} - (\varphi_1 G_1^{1/5} + \varphi_2 G_2^{1/5})}{G_{bl}^{1/5}} 100\% \quad (6)$$

The temperatures of relaxation transitions, namely,  $\beta$ -transition ( $T_\beta$ ), the glass transition ( $T_g$ ), and the liquid–liquid transition ( $T_{ll}$ ) were treated as a system of individual temperature points,<sup>21</sup> whereas segmental mobility was treated within the frame of the quantum model,<sup>21,22</sup> the basic subsystem of which is Kuhn's segment ( $M_s$ ). For the present subsystem, the fluctuation–dissipation theorem can be applied, which explains specific features of quantum transitions.

The main quantum number ( $S$ ) was found to vary for cooperative forms of the segmental mobility. These transitions were observed at:  $T_{coop}$ , unfreezing of cooperative mobility ( $S = 1$ );  $T_2$ ,  $\alpha_2$ -relaxation process ( $S = 2$ ), and  $T_{ll}$  ( $S = 3$ ). The number of states for Kuhn's segment characterized by four quantum numbers—radial ( $S_1$ ); azimuthal ( $S_2$ ); magnetic ( $S_3$ ); and spin ( $S_4$ )—can be found as follows:

$$Q = C_{m+k-1}^m \quad (7)$$

where  $C$  is the number of combinations;  $k$  is the sum of quantum numbers  $S_i$ ;  $k = 4$ ;  $m$  stands for the main quantum number  $S$ ;  $m = 1, 2, 3 \dots$

The Kuhn's segment value in the  $\beta$ -process range is:

$$M_s = M_e/Q = M_{e\beta}/4 \quad (8)$$

The value of  $M_s$  in the  $\alpha$ -process range is:

$$M_s \approx M_{e\alpha}/14 \quad (9)$$

where 14 is the number of states for Kuhn's segment over the temperature range  $T_{coop}$  to  $T_g$  since  $T_{ll} \cong T_g + 76^\circ\text{C}$ ; the temperature interval corresponding to one state change is  $12.5^\circ\text{C}$ .

Above  $T_{ll}$  temperature of the Kuhn's segment mobility is quasi-independent, so taking into account the ratio of molecular weight of Kuhn's segment components their diffusive interpenetration can be forecast at polymer blends' processing as a melt.<sup>25</sup>

## DSC

This method was used to analyze crystallization details of PA 12 in TPU. The investigation was done on a DSM-3A instrument (manufactured by the Institute of Biological Instruments of the Russian Academy of Sciences, Chernogolovka, Russia); the heating–cooling rate being  $16^\circ\text{C}/\text{min}$ . Samples of 6 mg were prepared by microtoming from the middle part of the injection molded bars measuring  $80 \times 10 \times 4$  mm. Virgin materials and their blends were tested. The melting–crystallization temperatures were determined from the maxima of corresponding peaks. The measurement error was  $\pm 0.5^\circ\text{C}$ . The relative crystallinity ( $C_{rel}$ ) was found using the expression:

$$C_{rel} = \frac{A_{bl}}{A_{PA\ 12}} \quad (10)$$

where  $A_{bl}$  and  $A_{PA\ 12}$  are the areas under the melting (crystallization) peaks of PA 12 in the blend under study and virgin PA 12, respectively.

## X-Ray Spectroscopy

X-ray measurements were performed on the wide-angle diffractometer DRON-3.0 (manufactured by AO "Nauczpribor," Orel, Russia). Copper  $K_\alpha$  radiation was used; the primary beam was nickel-filtered. The interplane distance in the crystal cell of PA 12 was determined by the location of the 200 peak maximum. Test specimens as plates measuring  $20 \times 10 \times 4$  mm were prepared just as

for the DSC analysis, i.e., they were cut from the middle part of the bars intended for impact testing.

The crystallinity of TPU/PA 12 blend samples was assessed following the procedure based on measuring the weight degree of the crystalline fraction ( $\alpha$ ) determined as the ratio of area occupied by the diffraction curve below the crystallization peaks to the sum of areas below these peaks ( $A_{cr}$ ) and that of an amorphous halo ( $A_{\alpha}$ )<sup>26</sup>:

$$\alpha = \frac{A_{cr}}{A_{cr} + A_{\alpha}} \quad (11)$$

To find deviations in the crystallinity degree (by weight) from its additive values, the crystallinity index ( $I_{cr}$ ), i.e., the ratio of a weight degree of crystallinity of the TPU/PA 12 blend sample to that of unmodified PA 12, was determined<sup>26</sup>:

$$I_{cr} = \frac{\alpha_{bl}}{\alpha_{PA\ 12}} \quad (12)$$

where  $\alpha_{bl}$  and  $\alpha_{PA\ 12}$  are values of crystallinity degree (by weight) for the blend and virgin PA 12.

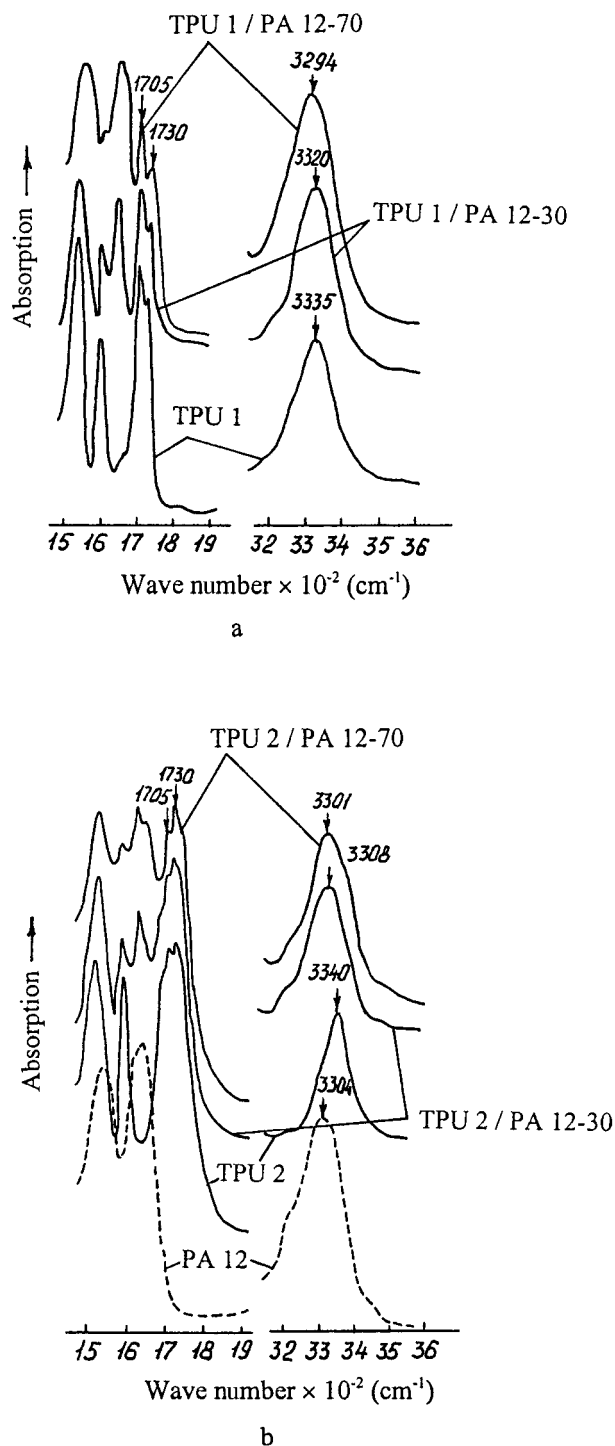
### Testing of Mechanical Properties

Mechanical strength of the materials was assessed in tensile and Charpy impact strength tests. The specimens were injection-molded using the temperature conditions optimal for TPU<sup>27</sup> (injection temperature,  $190 \pm 3^\circ\text{C}$ ; mold temperature,  $40 \pm 5^\circ\text{C}$ ; molding pressure,  $70 \pm 5\ \text{MPa}$ ). Tensile tests were done on dumbbell samples; the neck measured  $45 \times 5 \times 3\ \text{mm}$ . An Instron 1115 universal tensile testing machine (Instron Limited Corp., Buck, England) was operated at the speed of movable clamp 50 mm/min. In Charpy impact tests, bars measuring  $80 \times 10 \times 4\ \text{mm}$  were used. Small-angle undercuts on the specimens were made directly before testing. The tests were done on the pendulum testing machine PSW 1.5 (Werkstoff Prüfmaschinen, Leipzig, Germany) at  $23^\circ\text{C}$  and  $-40^\circ\text{C}$ . To determine impact strengths at negative temperatures, the samples were conditioned for 60 min in a cryogenic chamber of a special design;<sup>28</sup> then they were removed and tested immediately.

## RESULTS AND DISCUSSION

### IR-Spectral Analysis

Figure 1 shows IR spectra of TPU, PA 12, and their blends. In the A1 region, carbonyl absorp-



**Figure 1** IR spectra of virgin materials and blend compositions; PA 12 concentration is given in wt % in all Figures.

bency can be seen to split into two main bands with maxima at 1705 and 1730 cm<sup>-1</sup> [Fig. 1(a,b)]. In an earlier work,<sup>15,27</sup> the low-frequency shoul-

**Table II Effect of PA 12 Concentration on Optical Density Ratio for Bands in Carbonyl Absorption Region and Location of Maximum on Bands of Amine Group Valence Vibrations**

Blend Composition (wt %)	$D_{1705\text{ cm}^{-1}}/D_{1730\text{ cm}^{-1}}^{\text{a}}$	$D_{1705\text{ cm}^{-1}}/D_{1730\text{ cm}^{-1}}^{\text{b}}$	$\nu\text{NH (cm}^{-1}\text{)}$
TPU 1	1.20	1.18	3335
TPU 1/PA 12			
10	1.20	1.20	3320
30	1.21	1.24	3320
50	1.20	1.33	3310
70	1.19	1.32	3294
90	1.19	1.22	3294
PA 12			3304
TPU 2	0.87	0.89	3340
TPU 2/PA 12			
10	0.86	0.85	3340
30	0.87	0.83	3308
50	0.87	0.82	3298
70	0.86	0.76	3300
90	0.86	0.65	3298

PA 12, polyamide 12; TPU, thermoplastic polyurethanes; MVCIR, multiple violated complete internal reflection.

<sup>a</sup> Model optical blends, IR-spectra MVCIR.

<sup>b</sup> Real polymer blends, IR-absorption spectra.

der was related to absorption of self-associated carbonyl groups of the urethane fragment. At  $1730\text{ cm}^{-1}$ , absorption bands of free carbonyl groups of the urethane fragments are found along with low-energy hydrogen bonds (e.g., of dimers or trimers), and also of hydrogen bonds developing between NH group and oxygen in the oligoester block. The ratio of areas of the low-frequency part of A1 of the band to the total area, if the absorption coefficients are equal for associated and free carbonyl groups, represents a proportion of carbonyl groups associated with NH groups.<sup>15</sup>

The ratio of optical densities of bands at  $1705$  and  $1730\text{ cm}^{-1}$  can also show the self-association degree of urethane fragments.

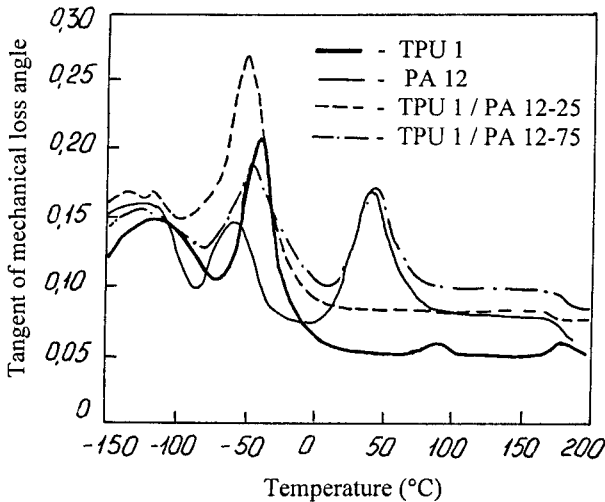
Addition of PA 12 is resulting in a variation of the shoulder intensity ratio in A1 band; the extent of this influence depends on the nature of TPU, elastomer, and concentration of the latter (Fig. 1, Table II). In "optical blends" which were obtained by putting PA 12 and TPU films on a surface of germanium crystal the  $D_{1705}/D_{1730}$  ratio is, in fact, constant being independent on a composition. Due to this, its variation in real blends results from the influence of elastomer on hydrogen interactions in TPU. Addition of PA 12 lowered the  $D_{1705}/D_{1730}$  ratio for ester-containing TPU 2, whereas for oligoether-containing TPU 1, it increased compared with the virgin thermo-

plastic elastomers. So, in blends with PA 12 the TPU 2, domain structure undergoes partial degradation whereas for TPU 1, the extent of microsegregation increases.

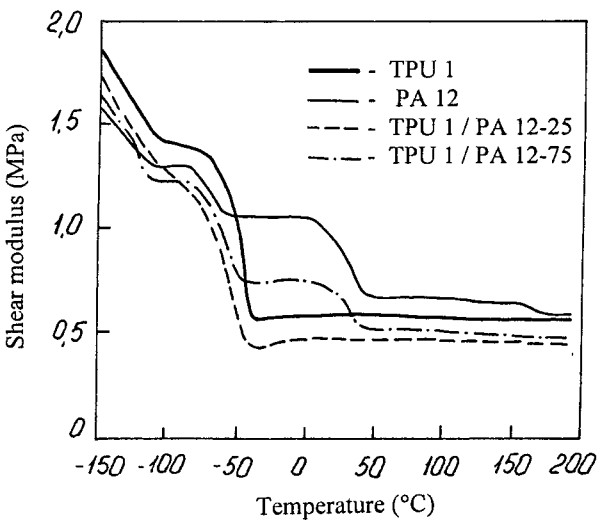
For the two TPU in blends with PA 12,  $\nu\text{NH}$  is usually shifted to the lower frequency region. At high concentrations ( $\geq 50\text{--}70\text{ wt \%}$  of PA 12) this band frequency is lower than that of the respective band in PA 12. Therefore, in blends with PA 12, more high-energy hydrogen bonds can be formed than that in the virgin components (PA 12 and TPU).

Comparison of calculated solubility parameters for thermoplastics and TPU individual blocks (Table I) showed a possibility to produce thermodynamically compatible blends of PA 12 with TPU 2 soft blocks as their solubility parameters differ by less than  $2.04\text{ (MJ/m}^3\text{)}^{0.5}$ .<sup>27</sup> Accordingly, it can be believed that the effect of the thermoplastic polymer on hydrogen bonding in TPU depends not only on its ability to hydrogen interaction with PA 12 macromolecules, but also on the distribution pattern of PA 12 in individual blocks.<sup>27</sup>

Parts of PA 12 chains can probably diffuse into the phase formed by the TPU 2 soft block leading to a partial degradation of self-associates in the hard block, because some of NH groups participated in formation of hydrogen bonds with both polyamide carbonyl groups and some of TPU car-



a



b

**Figure 2** Temperature dependence of  $\tan \delta$  (a) and shear dynamic modulus  $G$  (b) for PA 12, TPU 1, and their blends.

bonyl groups interacted with NH groups in PA 12. These rearrangements are most feasible in the interphase layers, the existence of which was suggested in a previous work.<sup>27</sup>

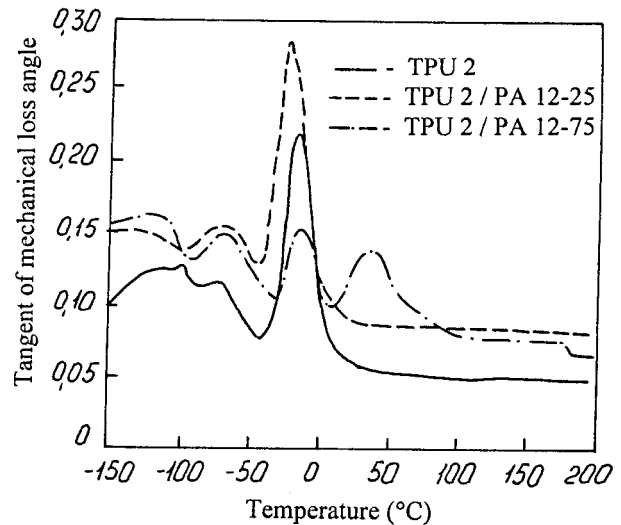
It is believed, therefore, that addition of PA 12 into segmented (thermoplastic) TPU helps the system of labile hydrogen bonds to rearrange, which fact must be considered when interpreting data on mechanical and other properties of the blends.

#### Relaxation Spectrometry Data

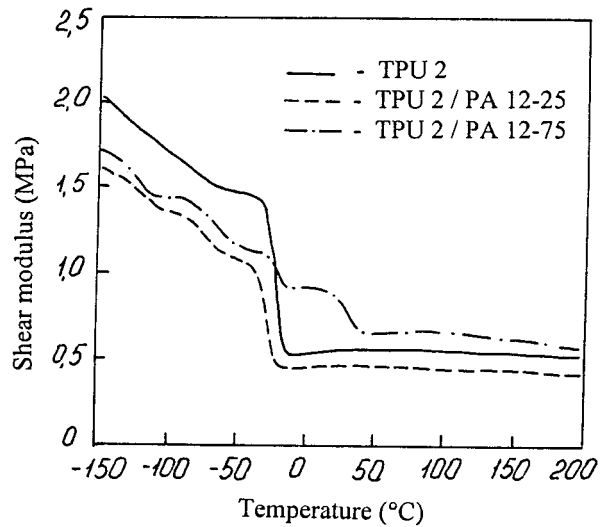
Figures 2 and 3 show temperature dependencies of  $\tan \delta$  and dynamic shear modulus for virgin

components and their blends. Tables III and IV list characteristics of relaxation transitions and the molecular structure.

There are three peaks on the temperature— $\tan \delta$  curve for virgin PA 12 (Fig. 2). The low-temperature  $\gamma$ -transition with a maximum at  $T_\gamma = -120^\circ\text{C}$  refers to the mobility of  $\text{CH}_2$  groups in the polyamide chain. The temperature—shear dynamic modulus curve has a plateau in the region of this process, the low-temperature boundary of which ( $T_{coop} = -110^\circ\text{C}$ ) can be taken as the initiation temperature of the cooperative molecular



a



b

**Figure 3** Temperature dependence of  $\tan \delta$  (a) and shear dynamic modulus (b) for TPU 2 and TPU 2/PA 12 blends.

**Table III Characteristics of Relaxation Transitions, Segmental Structure, and Interaction Energy for Virgin Polymers and TPU 1/PA 12 Blends**

Parameter	Relaxation Process												
	$\alpha$						$\beta$ ( $\gamma$ )						
	TPU 1/ PA 12 (15 wt %)	TPU 1/ PA 12 (25 wt %)	TPU 1/ PA 12 (50 wt %)	TPU 1/ PA 12 (75 wt %)	TPU 1/ PA 12	TPU 1/ PA 12	TPU 1/ PA 12 (15 wt %)	TPU 1/ PA 12 (25 wt %)	TPU 1/ PA 12 (50 wt %)	TPU 1/ PA 12 (75 wt %)	TPU 1/ PA 12	TPU 1/ PA 12	
Transition temperature ( $^{\circ}\text{C}$ )	-40	-35	-50	-52	-55	-55	(-110)	(-120)	(-130)	(-135)	(-125)	(-120)	
Dynamic segment $M_e$ (g/mol)	80	45	40	40	35	35						-60	
Kuhn's segment $M_s$ (g/mol)	3740				3900								(1000)
Reduced cohesive energy (kJ/mol)	270												1720
Interaction energy (kJ/mol)	38.0	50.7	52.6	57.4	62.2	67.0							
	40.1	41.0	41.5	46.8	50.7	71.0							

See Table II for abbreviations. In Tables III and IV, numerals in the second line of the "Transition temperature" column given for TPU/PA 12 blends characterize temperature values of respective transition in PA 12.



**Table IV Characteristics of Relaxation Transitions, Segmental Structure, and Interaction Energy for Pure TPU 2 and TPU 2/PA 12 Blends**

Parameter	Relaxation Process							
	$\alpha$				$\beta$ ( $\gamma$ )			
	TPU 2	TPU 2/ PA 12 (25 wt %)	TPU 2/ PA 12 (50 wt %)	TPU 2/ PA 12 (75 wt %)	TPU 2	TPU 2/ PA 12 (25 wt %)	TPU 2/ PA 12 (50 wt %)	TPU 2/ PA 12 (75 wt %)
Transition temperature ( $^{\circ}\text{C}$ )	-15	-25	-25 35	-18 35	(-110) -65	(-125) -75	(-127) -70	(-120) -62
Dynamic segment $M_e$ (g/mol)	3800				1420			
Kuhn's segment $M_s$ (g/mol)	355							
Reduced cohesive energy (kJ/mol)	63.6	62.8	65.6	64.2				
Interaction energy (kJ/mol)	61.5	51.0	67.3	66.7				

See Table II for abbreviations.

mobility. The dynamic segment (Table III) amounts to 1000 g/mol, which value equals to five monomer units of PA 12. The interaction energy within this plateau corresponds to Bondi cohesive energy (evaluated at a temperature of 0 K)<sup>29,30</sup> of PA 12 that describes the state of the frozen-out thermal mobility ( $E_{bl\ int} = 128$  kJ/mol,  $E_{coh} = 130$  kJ/mol). This allows treatment of the state of the Kuhn's segment within  $\gamma$ -process as transition from solid to conformable liquid, or in terms of quantum states as  $S_0$ - $S_1$  transition.

Beta-transition at  $T_{\beta}$  results from absorbed water<sup>31</sup> and unfrozen dipole-dipole and weak hydrogen bonds between chains. The dynamic segment for the plateau range of this process (Table III) reaches 9 monomer units. The interaction energy is 105.6 kJ/mol, which value approaches that of cohesive energy for polyamide at room temperature (106.8 kJ/mol). This plateau is supposed to be related to Kuhn's segment transition from the  $S_1$  to  $S_2$  state, and the upper temperature of the plateau equals  $T_2$ .

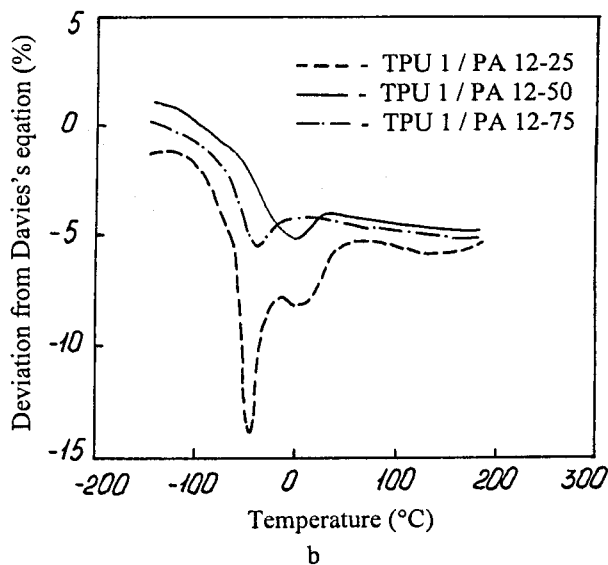
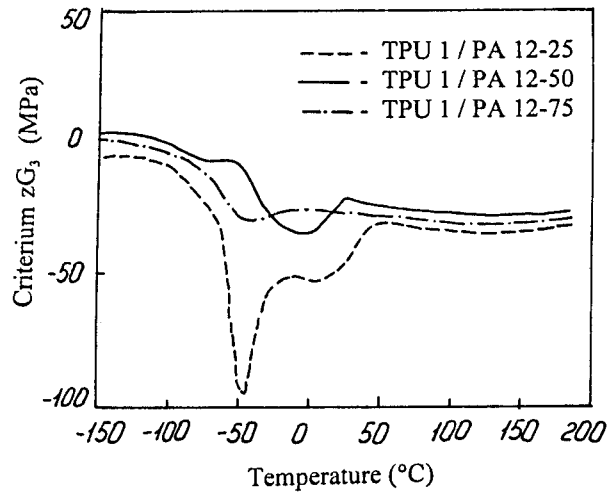
The third loss peak belongs to PA 12 glass transition at  $T_g = 35^{\circ}\text{C}$ . The dynamic segment within the high elasticity plateau is  $M_e = 3900$  g/mol; the interaction energy is 71 kJ/mol, which value approaches that of Bunn cohesive energy (evaluated at the boiling temperature)<sup>32</sup> viz 67 kJ/mol. From the quantum mechanics point of view, the transition of Kuhn's segments from conformable liquid to conformable gas  $S_2$ - $S_3$  was observed.

At  $T_{ll} = 135^{\circ}\text{C}$ , being approximately equal to polyamide crystallization temperature,<sup>33</sup> there was a small step in the shear dynamic modulus and a plateau, for which  $M_e = 5000$  g/mol. This corresponds with the critical molecular weight of PA 12 in the melt and the interaction energy is near Bunn cohesive energy.

In the range  $T_{coop}$ - $T_{ll}$  for PA 12, there is  $Q = T_{ll} - T_{\beta}/12.5 = 19.6$  states of Kuhn's segment, which is close to the theoretical value for a normal structure (for  $S = 3$ ;  $Q = 20$ ). The sizes of Kuhn's segment for  $a$  and  $ll$ -relaxation processes are given in Table III.

There are four temperature transitions on the temperature-tan $\delta$  curve for TPU 1 [Fig. 2(a)]. The transition at  $T_{\gamma} = -110^{\circ}\text{C}$  belongs to the mobility of aliphatic parts in the chain. The soft oligoether block in TPU 1 underwent the glass transition at  $T_{g\ sb} = -40^{\circ}\text{C}$ ; the hard block underwent the glass transition with a weak peak at  $T_{g\ hb} = 80^{\circ}\text{C}$ . The weak peak at  $175^{\circ}\text{C}$  is explained by the hard block mobility and TPU 1 transition to the visco-flow state. Kuhn's segment length in the soft block was 3.7 of the repeating units of oligoether. In the oligoether temperature range  $T_{ll}$ - $T_{coop}$ , there are 20 states with periodicity 6.25 $^{\circ}$ ; for the hard block the transition periodicity is 12.5 $^{\circ}$ .

Three major loss peaks were observed on the temperature-tan $\delta$  curve for TPU 2 [Fig. 3(a)]. The low-temperature transition at  $-100^{\circ}\text{C}$  refers to the unfrozen mobility of aliphatic fragments. Within the  $\beta$ -process associated with the ester

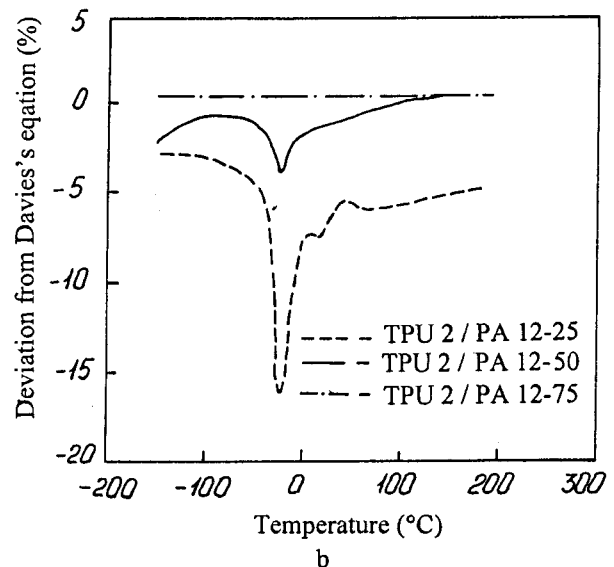
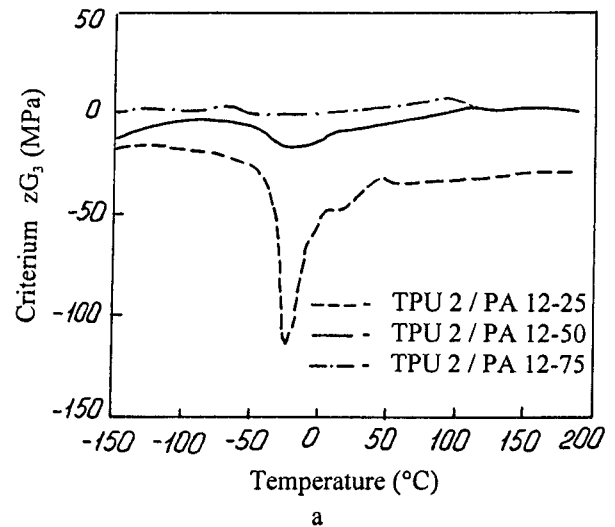


**Figure 4** Temperature dependence of  $zG_3$  (a) and deviation ( $\Delta$ ) from Davies equation (b) for TPU 1/PA 12 blends.

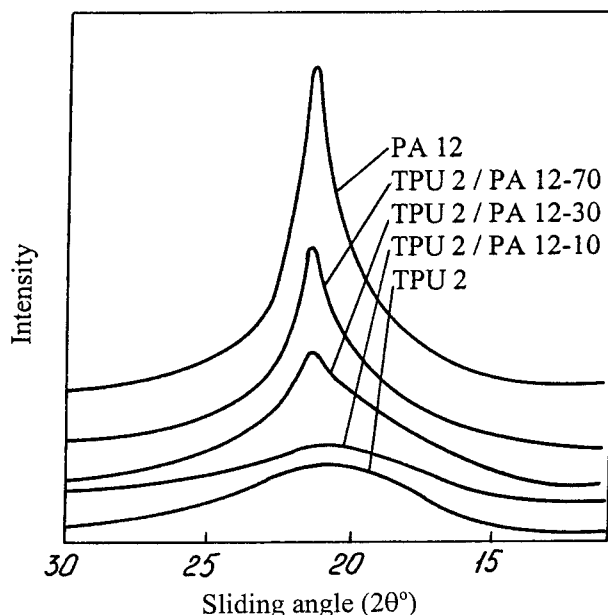
groups mobility, a plateau of a shear modulus is observed with  $T_{coop} = -65^\circ\text{C}$  [Fig. 3(b)]; the dynamic segment is 1420 g/mol. The soft TPU 2 block undergoes the glass transition at  $T_g = -15^\circ\text{C}$ . Kuhn's segment of oligoester is about 2.5 of repeating units; it has a transition periodicity multiple of  $6.25^\circ\text{C}$  just as oligoether in TPU 1.

Using dynamic mechanical spectroscopy, it was learned that virgin components show both normal (periodicity  $12.5^\circ\text{C}$ ) and fine (periodicity

$6.25^\circ\text{C}$ ) molecular structures. It is noted that above  $T_u$ , the Kuhn's segment mobility is quasi independent (state of conformable gas). Therefore, the Kuhn's segment can be assumed as the major kinetic unit that determines (or influences) diffusive processes in the molten polymer blend. With this in view, one can expect that as the  $M_s$  value for the TPU 2 soft block (Table IV) exceeds the  $M_s$  value for PA 12, its diffusion into PA 12 is limited. However, PA 12 can diffuse into the TPU



**Figure 5** Temperature dependence of  $zG_3$  (a) and deviations from Davies equation (b) for TPU 2/PA 12 blends.



**Figure 6** Intensities on X-rays scattered at wide angles by specimens of TPU 2, PA 12, and TPU 2/PA 12 blends.

2 soft block. The close size of PA 12 Kuhn's segments and the TPU 1 soft block (Table III) presume feasibility of their mutual diffusion.

In TPU/PA 12 blends, the TPU transition temperatures do not depend on their compositions (Figs. 2 and 3, Tables III and IV). In TPU 1/PA 12 blends, the transition temperatures  $T_{g\ sb}$  and  $T_{\beta}$  of PA 12 can be written by analogy with Fox relationship that describes the temperature dependence of the glass transition for compatible blends.<sup>26</sup>

$$1/T_{g\ sb\ bl} = \varphi_1/T_{g\ sb\ TPU} + \varphi_2/T_{\beta\ PA\ 12} \quad (13)$$

where  $\varphi_1$  and  $\varphi_2$  are the weight shares of soft block of TPU and PA 12 in the hypothetical blend containing only these components.

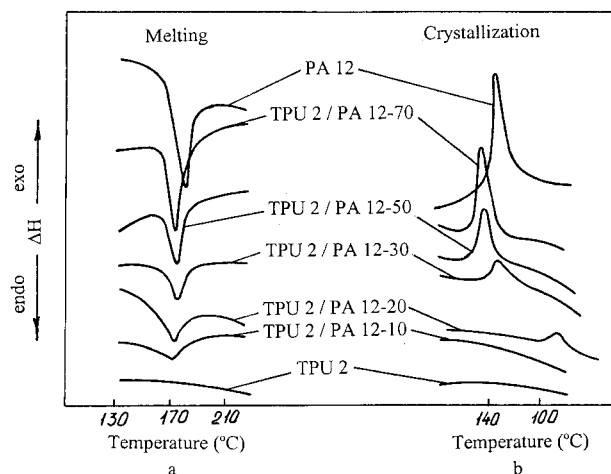
The glass transition temperature of PA 12 increases by 10°C if its contents in the blend decreases (Table III). This can be explained by the influence of interchain interaction with hard block owing to PA 12 diffusion into the oligoether block. Therefore, the extent of microsegregation in TPU 1 in the presence of PA 12 can increase, as was shown from IR-spectroscopy data.

Unlike TPU 1, for TPU 2 eq. (13) is complying only for PA 12 concentrations  $\leq 25$  wt %. The size of Kuhn's segment ( $M_s$ ) for the soft PA 12 block is less than that for polyester soft block; therefore, from kinetic considerations the diffusion on the segmental level is only possible for PA 12 into TPU 2 soft block. For 50 wt % and 75 wt % of PA 12, eq. (13) is not fulfilled, compatibility decreases, which is supported by the constant  $T_g$  value for PA 12 (Table IV). The  $G$ -concentration dependence now follows the Davies equation (Figs. 4,5), which is valid for the blends with the two-phase continuity. For the given concentrations, the interaction energy corresponds to the additive contribution of the components. In contrast, all blends based on TPU 1 and TPU 2 complying eq. (13) have interaction energies below the additive value (Tables III and IV). In compatible blends, PA 12 softens TPU, which is shown by a lower  $T_{g\ sb}$  or  $\beta$ -transition temperature in TPU (Tables III and IV). The highest losses of interactions in blends, evaluated from the  $zG_3$ -temperature dependence, and deviations from Davies equation, were observed at the glass transition temperature of the oligoester block for all test blends, which showed partial compatibility described by eq. (13). For TPU 1-based blends lowering in  $zG_3$  value decreases with increasing PA 12 contents at a given temperature. The softening effect of thermoplastic polyurethanes in the blend intensifies, thus making the microsegregation of hard blocks easier and shows in most associated urethane groups in TPU 1 hard block, as was

**Table V** Effect of PA 12 Concentration on Crystallinity Index  $I_{cr}$  in TPU 2/PA 12 Blends Calculated from Equation 12 and Based on X-Ray Spectroscopy

Index of Crystallinity	Value of Parameter Vs PA 12 Concentration (wt %)								
	0	10	20	30	40	50	70	90	100
$I_{cr}$ (Relative unit)	0	0.08	0.16	0.26	0.30	0.42	0.66	0.84	1.0
$I_{cr}^*$ (Relative unit)	0	0.1	0.2	0.3	0.4	0.5	0.7	0.9	1.0

See Table II for abbreviations.  $I_{cr}^*$ , additive values for crystallinity index calculated based on a share of components that do not interfere.



**Figure 7** Differential thermal curves of melting (a) and crystallization (b) of TPU 2, PA 12, and TPU 2/PA 12 blends.

detected by IR-spectroscopy technique (Fig. 1, Table II). For TPU 2-based blends, when polyamide content was increased, phases separated, the softening effect diminished, and the formed boundary between phases hindered the microsegregation, which showed in fewer associated functional groups present in the urethane part of the hard block, as detected by IR-spectroscopy technique (Fig. 1, Table II).

### Study of the Structure

#### Wide-Angle Radiography

Figure 6 shows a diffractogram for PA 12. There is one reflex at  $2\theta = 21^\circ 17'$  (interplane distance  $d = 4.18 \text{ \AA}$ ). Kazaryan et al.<sup>34</sup> stated that polyamides could crystallize to give hexagonal structure ( $\gamma$ -type). The radiograph has one reflex at  $2\theta$

$= 21^\circ 5'$  ( $d = 4.13 \text{ \AA}$ ). PA 12 has the monoclinic structure. Nevertheless, the diffraction angles of reflexes 200, 020, and 220 are close to each other (a chain axis is axis  $C$ ), so that all three reflexes fuse into one and the cell becomes a pseudo hexagonal.

The wide-angle radiography found that TPU 2, just as TPU 1, is amorphous: their diffractograms show only halos of an amorphous scattering (Fig. 6).

Diffractograms of TPU/PA 12 blends have clearly pronounced PA 12 reflexes at  $2\theta = 21^\circ 17'$  and an amorphous halo for TPU with a maximum at  $2\theta = 20\text{--}21^\circ$  (Fig. 6). As PA 12 content increases, its diffraction peak becomes more intensive (more sharp). The angular location of the reflex maximum remained unchanged. The crystal lattice parameter remained in fact unchanged ( $4.18 \text{ \AA}$ ). Consequently, cooling of the molten blend initiates PA 12 crystals, which grew within a TPU amorphous phase without involving macromolecules of the latter into the crystallite composition. Therefore, the above arguments about probable compatibility of components refer mainly to the amorphous part of PA 12.

The concentration–crystallinity index dependence showed the specific feature of the blends to be the decrease in the PA 12 crystallinity as compared with the additive values (Table V). This is especially typical for PA 12 contents below 50 wt %, i.e., of the blends, in which TPU 2 is the dispersion phase. Similar observations were obtained for TPU 1/PA 12 blends.

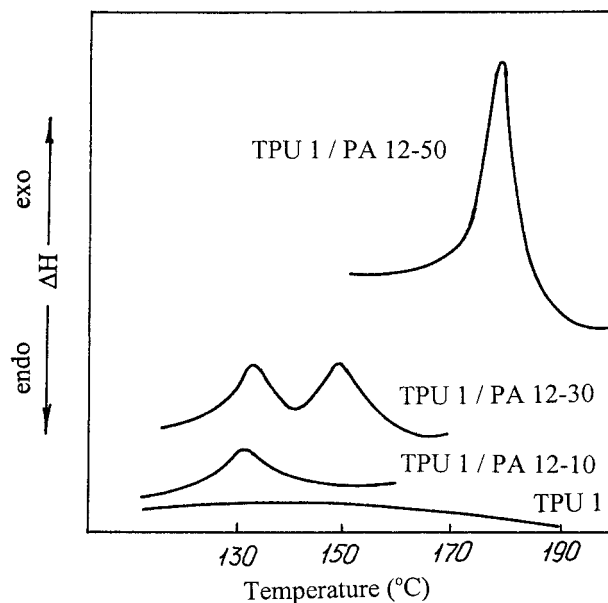
#### DSC Data

Figure 7 shows PA 12 to melt at  $T_m = 179^\circ\text{C}$  at the experimental conditions and it crystallizes at  $T_{cr} = 133^\circ\text{C}$ . For TPU 2/PA 12 blends, the melting

**Table VI** Temperatures of Transitions and Relative Crystallinity  $C_{rel}$  Calculated from Equation 10 for PA 12 in TPU 2/PA 12 Blends (Dynamic Scanning Calorimetry Data)

Parameter	Value of Parameters Vs PA 12 Concentration (wt %)								
	0	10	20	30	40	50	70	90	100
$T_m$ (°C)		173	173	173	173	175	175	179	179
$T_{cr}$ (°C)			84	138	138	141	141	141	133
$\Delta T = T_m - T_{cr}$ (°C)			41	35	35	34	34	38	46
$C_{rel}$ (Relative unit)	0	0	0.028	0.21	0.27	0.43	0.7	0.9	1.0
$C_{rel}^*$ (Relative unit)	0	0.1	0.2	0.3	0.4	0.5	0.7	0.9	1.0

See Table II for abbreviations.  $C_{rel}^*$  additive values for relative crystallinity calculated based on a share of components that do not interfere.



**Figure 8** Differential thermal curves of the TPU 1/PA 12 blend crystallization.

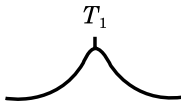
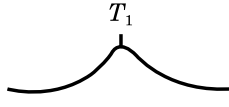

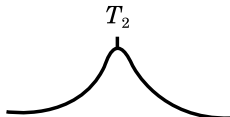
temperature was decreased by 5–7°C as compared with the homopolymer (Fig. 7). No crystallization was detected in PA 12 if the blend contained 10 wt % of PA 12 by using DSC technique. For 20 wt % of PA 12,  $T_{cr}$  was lower by 49°C, whereas for blends with 30–90% of polyamide,  $T_{cr}$  was higher by 5–8°C as compared with pure PA

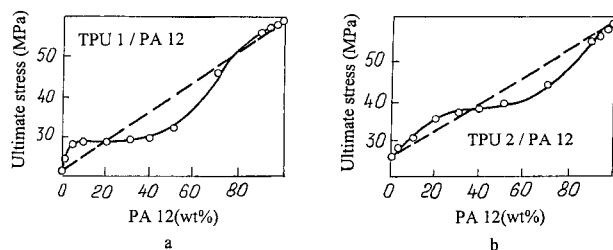
12 (Fig. 7, Table VI). The difference between  $T_m$  and  $T_{cr}$  ( $\Delta T$ ) was lower for blends than for unmodified (virgin) PA 12 (Table VI). MacKnight et al.<sup>26</sup> stated that lower  $\Delta T$  in a blend implies the more ordered molecular structure in the blend in contrast to virgin polymers. The concentration—the relative crystallinity degree dependencies obtained for blends by DSC procedure are in correlation with the mode of crystallinity index variations (Tables V and VI).

Comparison of data in Figures 7 and 8 and Tables VI and VII show that TPU nature and PA 12 contents strongly influence its crystallization in the blends. For TPU 1 blended with 30 wt % PA 12 (Fig. 8), unlike other blends, two crystallization peaks (low- and high-temperature peaks) are found.  $T_{cr}$  values for the low-temperature peak are actually equal to  $T_{cr}$  of PA 12; for the high-temperature peak they exceed  $T_{cr}$  for PA 12 by 16–18°C.  $T_m$  of PA 12 in TPU 1/PA 12 blends varied less than in TPU 2/PA 12 blends (Tables VI and VII).

Comparison of the wide-angle radiography and the DSC findings (Figs. 6, 7, and 8) showed that changes in crystallization curves with TPU concentration and composition, are of kinetic origin and do not involve formation of a specific crystalline structure of PA 12 in the blends. This is also supported by the fact that no changes occurred in the melting peak patterns on the differential

**Table VII** Differential Thermal Curves of Crystallization and Temperatures of Phase Transitions for PA 12 in TPU 1/PA 12 Blends from Dynamic Scanning Colorimetry Data

Material	Curve	$T_{cr}$ (°C)	$T_m$ (°C)	$\Delta T = T_m - T_{cr}$ (°C)
TPU 1/PA 12–10 wt %		$T_1 = 133$	177	44
TPU 1/PA 12–20 wt %		$T_1 = 134$	177	43
TPU 1/PA 12–30 wt %		$T_1 = 134$ $T_2 = 149$	179	45
TPU 1/PA 12–50 wt %		$T_2 = 151$	179	28



**Figure 9** Effect of PA 12 content on ultimate tensile stress for TPU/PA 12 blends; dashed lines stand for additive values.

thermal curves obtained by the DSC technique (Figs. 6 and 7) for the blends of a different content.

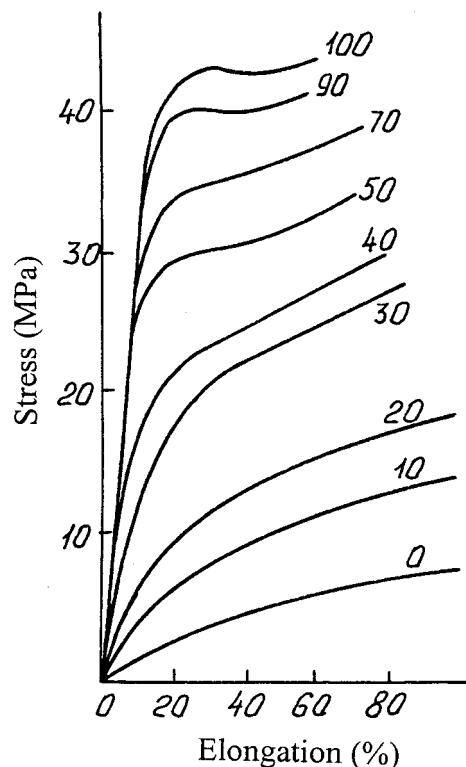
Consider observed variations during thermoplastic polyurethanes crystallization in view of earlier findings on compatibility and interphase interactions in the test blends. A common feature of the tested blends is a decrease in crystallization of PA 12 compared with the additive values. This is especially typical of the crystallizable component contents below 50 wt %, i.e., blends with a TPU dispersion phase. Slower crystallization of PA 12 in blends could be explained by formation of interphase (transient) layers owing to diffusion when the blending melts. In these layers, molecular mobility is limited, thus hampering macromolecular folding because of intensive intermolecular (adhesional) interaction. As a result, some part of a crystalline phase can become amorphous.<sup>26</sup> Because linear polymers have the chain structure, the mobility limitations can affect not only macromolecules directly participating in intermolecular interactions, but also layers found at a considerable distance from the interphase interface.<sup>26</sup>

In TPU/PA 12 blends, intensive intermolecular interactions take place and compatibility is feasible for PA 12 amorphous phase and TPU 2 soft block owing to thermodynamic considerations, or TPU 1 soft block owing to kinetic considerations; this results in two consequences. On the one hand, in the interphase regions, owing to intensive interphase interactions, sites of PA 12 micro orientation occur, which can act as crosslinking centers and promoters crystallization. This could probably give an increase in PA 12 crystallization temperature in the blends (Figs. 7 and 8; Tables VI and VII). On the other hand, because of intensive intermolecular interaction, PA 12 molecular mobility is limited, which decreases molecular mobility and a rate of the crystallization process.

As the result, PA 12 crystallinity decreases in the blends in contrast with homopolymer.

The weaker effect of a TPU phase on PA 12 crystallization with its contents above 50 wt % can be explained, as will be described below, by the phase inversion and formation of a dispersion phase by the TPU. As a result, the surface area and interphase region portion in the total volume of the blend decrease along with their effect on crystallization. It may be assumed that in TPU 2/PA 12 blends containing up to 20 wt % of polyamide and characterized by a presence or an absence of a single low-temperature crystallization peak, the role of interphase interaction is so great that a PA 12 phase transfers completely into the "interphase state." To crystallize PA 12, severe overcooling (by 49°C) of the blend is needed as compared with PA 12 (Table VI). Also, of the  $T_{cr}$  of PA 12 in TPU 2/PA 12 (20 wt %) blends is by 50°C lower, in contrast to TPU 1/PA 12 (20 wt %) (Tables VI and VII), come from stronger interphase adhesion and improved compatibility in TPU 2/PA 12 blends.

At high contents of PA 12 (> 30 wt %),  $T_{cr}$  of PA 12 in TPU 1/PA 12 blends increased more signif-



**Figure 10** Stress-strain curves for TPU 2/PA 12 blends. Numerals on curves stand for PA 12 contents.

**Table VIII** Effect of PA 12 Concentration on Relative Elongation at Break and Hardness of TPU/PA 12 Blends

PA 12 Concentration (wt %)	Relative Elongation at Break (%)		Shore (A) Hardness (Relative Unit)	
	TPU 2/PA 12	TPU 1/PA 12	TPU 2/PA 12	TPU 1/PA 12
0	270	225	83	82
10	265	320	87	86
20	210	280	88	87
30	160	250	92	89
40	150	130	94	91
50	90	110	96	93
60	85	90	96	94
70	80	85	96	94
80	80	80	96	94
90	80	80	—	—
100	75	75	—	—

See Table II for abbreviations.

icantly than in TPU 2/PA 12 blends (Tables VI and VII). This can probably be explained by improved compatibility revealed by the relaxation spectroscopy technique in TPU 1/PA 12 blends in contrast to TPU 2/PA 12 blends. As a result, PA 12 crystallization initiated by reorienting macromolecular fragments participating in interphase interactions takes place in TPU 1/PA 12 blends at weaker overcooling of the melt.

### **Mechanical Properties of the Blends**

Figures 9 and 10 and Table VIII show concentration dependencies of some properties for blends subjected to tensile testing. All tested blends showed deviations in mechanical properties from their additive values. The pattern of the dependence is influenced by the thermoplastic elastomer origin. The mechanical strength values exceed the additive ones for PA 12 low contents (up to 20 wt % for TPU 1/PA 12 blends and up to 30 wt % for TPU 2/PA 12 blends), i.e., when PA 12 is as the dispersion phase. Now the deformation behavior of the compositions does not change substantially (Fig. 10; Table VIII). TPU 1/PA 12 blends show somewhat increased relative elongation at break as compared with the virgin TPU 1. Significant decrease in the blend deformability was observed at TPU contents above 30–40 wt % (Fig. 10, Table VIII), i.e., the concentrations characterized by the phase structure inversion.<sup>35</sup> Increasing further the PA 12 contents caused monotonic variations in the values.

The stress-strain curves show the inclination angle of the strain curve, first, to increase (com-

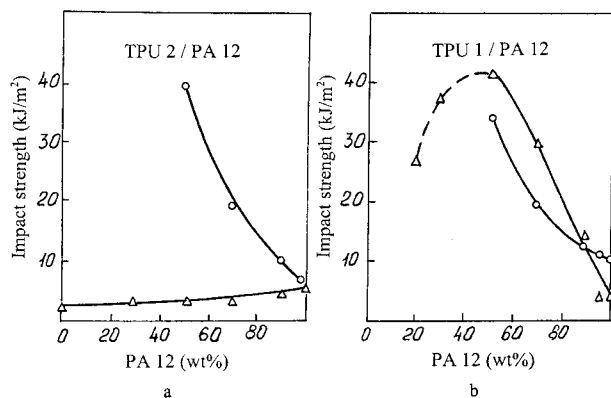
pared with pure TPU) with increasing the PA 12 contents (Fig. 10). At low strains, considerable improvements in strength (several times) of the blends were observed in contrast with the base TPU. With thermoplastic polyurethane contents above 40 wt %, the inclination angles of the strain curves did not change much, which was explained by PA 12 involved in the deformation process and forming the continuous phase.

Comparison of mechanical testing results with those of structural analysis revealed certain correlations between structural parameters and mechanical properties. Probably, differences in the pattern of the dependence of mechanical strength of the blend on the TPU contents (at concentrations  $\leq 30$ – $40$  wt % and  $> 40$  wt %) are because of different degrees of its dispersion, changes in conditions of forming of interphase layers, and smaller contributions in structure-mechanical characteristics with increasing PA 12 contents.

Differences in mechanical properties of the blends, containing up to 30 wt % of TPU, may result from characteristic features of a structure and intermolecular interactions of components in the interphase layers.

Modification by using a thermoplastic polymer allowed a varied hardness interval of the blends; but TPU concentration above 40 wt % increased hardness only slightly (Table VIII).

Phase-structural variations considerably influence the behavior of blend systems under impact loading (Fig. 11). At a PA 12 concentration  $\leq 40$  wt % and 23°C, the test specimens withstood the impact loading, which fact can be explained by a



**Figure 11** Effect of PA 12 concentration on impact strength of the blends at testing temperatures: 23°C (○) and -40°C (Δ); (- - -) stands for unbroken specimens.

lack of a continuity in the thermoplastic phase. Differences in the impact resistance at low temperatures of TPU-based blends result from much lower glass transition temperature of the TPU soft block in the oligoether-based TPU 1 in contrast to the oligoester-based TPU 2.

## CONCLUSIONS

The addition of PA 12 into segmented TPU causes rearrangement in the system of labile hydrogen bonds, the nature of which depends on the polyurethane origin. For ester-based TPU (TPU 2), the extent of domain microsegregation decreased during blending. On the contrary, in oligoether-based TPU (TPU 1), the microphase separation was more pronounced when PA 12 was added. IR-spectroscopy showed the two TPU versions blended with PA 12 to form more high-energy hydrogen bonds with polyamide macromolecules than in homopolyurethanes.

In blends of partial compatibility, miscibility was observed between PA 12 and a microphase formed by the TPU soft block. In ester-TPU-based blends, miscibility can be achieved owing to close solubility parameters (solubility parameters differ by 1.2 (MJ/m<sup>3</sup>)<sup>0.5</sup> between the soft block of TPU 2 and PA 12). When oligoether-based TPU 1 was mixed with PA 12, the miscibility was improved owing to the close sizes of Kuhn's segments in the polyurethane soft block and polyamide. Therefore, although thermodynamic preconditions are less favorable with TPU 1 than with TPU 2 [solubility parameters of the TPU 1 soft block and PA 12 differ by 4.7 (MJ/m<sup>3</sup>)<sup>0.5</sup>], a

partial compatibility in TPU 1/PA 12 blends can be achieved at wider variations in the component contents than in TPU 2/PA 12 blends. Partial compatibility of PA 12 with the TPU soft block is followed by the latter plasticization this shifts by  $\approx 15^\circ\text{C}$  the glass transition temperature of the soft block to the lower-temperature region. PA 12 was crystallized in both tested blends without much variation of the polyamide crystal lattice parameters. It may be assumed that only the amorphous portion of polyamide or interphase layers with irregular arrangement participate in interphase interactions with TPU. Intensive interphase interactions lead to slower crystallization of PA 12 in the blends where it is as the dispersion phase and, in contrast, to faster crystallization if polyamide is as the polymer matrix.

Addition of PA 12 to TPU provides wide variations in the polyurethane mechanical strength and hardness. At low concentrations of PA 12 (up to 20–30 wt %), mechanical strength values for the blends were higher than additive ones. Blends containing TPU of 30–50 wt % belong to the impact resistant group; TPU1/PA 12 compositions showed higher impact resistance at low-temperature ( $-40^\circ\text{C}$ ) testing, than TPU 2/PA 12; this can be explained by the lower glass transition temperature of the TPU 1 soft block as compared with TPU 2.

## REFERENCES

1. Ratzch, M.; Haudel, G.; Pompe, G.; Neyer, E. *J Macromol Sci Chem* 1990, A27, 1631.
2. Zhu, Y. Q.; Huang, Y. J.; Chi, Z. G. *J Appl Polym Sci* 1995, 56, 1371.
3. Chiang, W. Y.; Huang, C.-Y. *J Appl Polym Sci* 1989, 38, 951.
4. Banhegyi, G.; Karasz, F. E. *J Appl Polym Sci* 1990, 40, 435.
5. Petrovic, Z. S.; Byolinski-Simendic, J.; Divjakovic, V. *J Appl Polym Sci* 1991, 42, 779.
6. Kober, M.; Wesslen, B. *J Appl Polym Sci* 1994, 54, 793.
7. Yang, C. Z.; Zhang, X.; Oconnell, E. M.; Goddard, R. J.; Cooper, S. L. *J Appl Polym Sci* 1994, 51, 365.
8. Lorenz, G.; Klee, D.; Hocker, H.; Mittermayer, C. *J Appl Polym Sci* 1995, 57, 391.
9. Kercha, Yu. Yu. *Physical Chemistry of Polyurethanes* (in Russian); Naukova Dumka: Kiev, 1979.
10. Buist, J. M. *Developments in Polyurethane* (Russian translation); Khimia: Moscow, 1982.
11. Seymor, R.; Estes, G.; Cooper, S. *Am Chem Soc Polym Eng Prepr* 1970, 11, 867.



12. Vatulev, V. N.; Laptii, S. V.; Kercha, Yu. Yu. IR-Spectra and Structure of Polyurethanes (in Russian); Naukova Dumka: Kiev, 1978.
13. Askadsky A. A.; Matveev, Yu. I. Chemical Structure and Physical Properties of Polymers (in Russian); Khimia: Moscow, 1983.
14. Sung, C. S. P.; Hu, C. B. *Macromolecules* 1981, 14, 212.
15. Volkov, V. G.; Nelson, K. V.; Sotnikova, E. N. *J Appl Spectrosc* (in Russian) 1982, 36, 787.
16. Treloar, L. *The Physics of Rubber Elasticity* (Russian translation); Inostrannaya literatura: Moscow, 1953.
17. Nemilov, S. V. *USSR Acad Sci Rep* (in Russian) 1980, 291, 147.
18. Fedorov, V. D.; Polosmak, N. D.; Shcherbakov, S. V. *BSSR Acad Sci Trans, Phys-Technol Ser* (in Russian) 1983, 2, 30.
19. Perepechko, I. I. *USSR Acad Sci Rep* (in Russian) 1986, 291, 1.
20. Davies, W. E. A. *Phys D Appl Phys* 1971, 4, 318.
21. Lushcheikin, G. A. In *Systems of Special Temperature Points for Solids* (in Russian), Venevcev, Y. N.; Muromcev, Y. I., Eds.; Nauka: Moscow, 1986; p. 68.
22. Fedorov, V. D. *BSSR Acad Sci Rep* (in Russian) 1989, 33, 1008.
23. Levich, V. G.; Vdovin, Yu. A.; Myamlin, V. A. *Course on Theoretical Physics* (in Russian); Nauka: Moscow, 1971; p. 2.
24. Smirnov, A. P. In *Systems of Special Temperature Points for Solids* (in Russian), Venevcev, Y. N.; Muromcev, Y. I., Eds.; Nauka: Moscow, 1986; p. 210.
25. Fedorov, V. D.; Koval, V. N.; Pesetskii, S. S. *BSSR Acad Sci Trans, Phys Technol Ser* (in Russian) 1997, 3, 7.
26. MacKnight, W. J.; Karasz, F. E.; Fried, J. R. In *Polymer Blends*; Paul, D.; Newman, S., Eds.; Academic: New York, 1977; p. 1.
27. Pesetskii, S. S.; Polosmak, N. D.; Malinin, L. N.; Koval, V. N. *BSSR Acad Sci Rep* (in Russian) 1990, 34, 616.
28. Pesetskii, S. S.; Jurkowski, B.; Storozcuk, I. P.; Koval, V. N. *J Appl Polym Sci*, 1989, 74, 490.
29. Bondi, A. *J Chem Eng Data* 1963, 8, 371.
30. Bondi, A. *J Polym Sci* 1964, A2, 3159.
31. Varlet, J.; Cavaille, J. Y.; Perez, J. *J Polym Sci* 1990, 28, 2691.
32. Bunn, C. W. *J Polym Sci* 1955, 16, 323.
33. Bershtein, V. A.; Egorov, V. M. *DSC in Physical Chemistry of Polymers* (in Russian); Khimia: Leningrad, 1990.
34. Kazaryan, L. G.; Zezina, L. A.; Vasiliev, N. I.; Ivanova, L. *Vysokomol Soedin* (in Russian) 1989, 31A, 1650.
35. Pesetskii, S. S.; Polosmak, N. D.; Koval, V. N.; Kaplan, M. B. *BSSR Acad Sci Trans, Phys Technol Ser*, 1991, 1, 40.